

## CHAPTER 10

---

# Hemolysin E (HlyE, ClyA, SheA) and Related Toxins

Stuart Hunt, Jeffrey Green and Peter J. Artymiuk\*

### Abstract

Certain strains of *Escherichia coli*, *Salmonella enterica* and *Shigella flexneri* produce a pore-forming toxin hemolysin E (HlyE), also known as cytolysin A (ClyA) and silent hemolysin, locus A (SheA). HlyE lyses erythrocytes and mammalian cells, forming transmembrane pores with a minimum internal diameter of ~25 Å. We review the current knowledge of HlyE structure and function in its solution and pore forms, models for membrane insertion, its potential use in biotechnology applications and its relationship to a wider superfamily of toxins.

### Introduction

Hemolysin E (HlyE; also known as ClyA or SheA) is a novel, pore-forming toxin synthesized by *Escherichia coli* and other enteric bacteria.<sup>1-6</sup> HlyE lyses mammalian erythrocytes, is cytotoxic toward cultured mammalian cells, induces apoptosis in macrophages and has been reported to induce slow intracellular Ca<sup>2+</sup> oscillations in epithelial cells.<sup>7,8</sup> Genes coding for close homologues are present in the genomes of *Salmonella enterica* serovar Typhi or serovar Paratyphi A and *Shigella flexneri*, the causative agents of typhoid fever, paratyphoid and dysentery respectively.<sup>9</sup> In addition, a more distantly related HlyE occurs in avian *E. coli* strains<sup>10,11</sup> which lack the more widely studied RTX pore-forming hemolysins.<sup>12</sup> Indeed, evidence to date suggests that the *hlyA* gene, encoding the RTX protein HlyA, that is an established virulence factor in extraintestinal *E. coli* infections is not found in *E. coli* strains that possess *hlyE*.<sup>13</sup> Recently it has been shown that antibodies to HlyE are present in humans that have been infected with either *S. Typhi* or *S. Paratyphi A* and that *hlyE* is expressed in *S. Typhi* infected human macrophages, where it is thought to constrain bacterial growth and thereby contribute to chronic infection.<sup>14</sup> Furthermore, following the demonstration that all wild-type *S. Typhi* and *S. Paratyphi A* strains tested so far possess functional HlyE proteins it has been suggested that HlyE plays a role in pathogenesis of these bacteria.<sup>15,16</sup> However, *hlyE* is apparently not associated with sudden infant death syndrome<sup>17</sup> and screening for the presence of functional *hlyE* genes suggests that is likely to act as a virulence factor in a relatively small group of Enterobacteriaceae.<sup>18</sup>

### Regulation of *hlyE* Expression

Regulation of *hlyE* expression in *E. coli* K-12 is complex and is influenced by several environmental signals. A single site in the *hlyE* promoter enhances expression in response to oxygen starvation when occupied by FNR (regulator of Fumarate Nitrate Reduction)<sup>2,19</sup> and in response to glucose-starvation when occupied by CRP (cAMP receptor protein).<sup>19,20</sup> In addition, the

---

\*Corresponding Author: Peter J. Artymiuk—The Krebs Institute, Department of Molecular Biology and Biotechnology, University of Sheffield, Sheffield, S10 2TN, UK.  
Email: p.artymiuk@sheffield.ac.uk

nucleoid structuring protein H-NS has a negative effect on FNR-driven *hlyE* expression and a positive effect on CRP-driven *hlyE* expression.<sup>19,20</sup> Furthermore, H-NS-mediated repression is antagonized by a fourth transcription factor, SlyA, that responds to amino acid starvation.<sup>3,19,21,22</sup> In *S. Typhi* expression of *hlyE* is activated by the PhoPQ two-component system that is also responsible for the regulation of many genes expressed during host infection, but not by SsrB.<sup>14</sup> The effects of other transcription factors, such as those known to regulate *hlyE* expression in *E. coli*, have not yet been tested in *Salmonella*.

## Structural Studies on HlyE

### *Crystal Structure of the Water-Soluble Form*

The X-ray crystal structure of the water-soluble form of HlyE shows that it is a 34 kDa rod-shaped molecule consisting of a bundle of four long (80-90 Å) helices, which coil around each other with significant elaborations at both poles of the four-helix bundle (Fig. 1).<sup>9</sup> In the tail domain, which contains the N- and C-terminal regions of the protein, a shorter (30 Å) helix ( $\alpha$ G) packs against the four long helices, forming a five-helix bundle for about one third of the length of the molecule. Random and site-directed mutagenesis has revealed that residues in the  $\alpha$ G region play important roles in HlyE activity.<sup>23,24</sup> HlyE possesses only two cysteine residues and the crystal structure revealed that these are positioned very close to each other in the tail domain<sup>9</sup> (Fig. 1) and can be oxidized to form a disulphide bond.<sup>23,25</sup> It has been reported that the

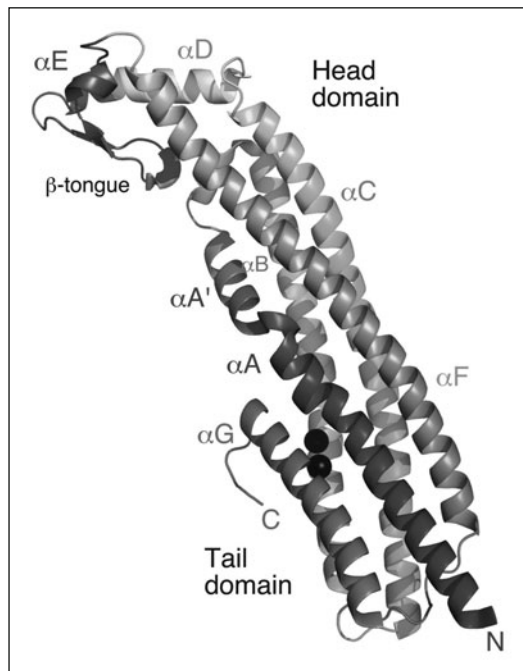


Figure 1. Three-dimensional structure of HlyE. The backbone fold of the HlyE monomer is shown in cartoon representation, rainbow coloured from blue (N-terminal, labelled N) to red (C-terminal, labelled C), except for the hydrophobic region (residues 177-203) which is coloured grey. The head and tail domains are indicated and helices A to G are labelled, together with the beta tongue region. The two cysteine residues are shown as black spheres. Produced using PyMol.<sup>48</sup> A color version of this image is available at [www.landesbioscience.com/curie](http://www.landesbioscience.com/curie).

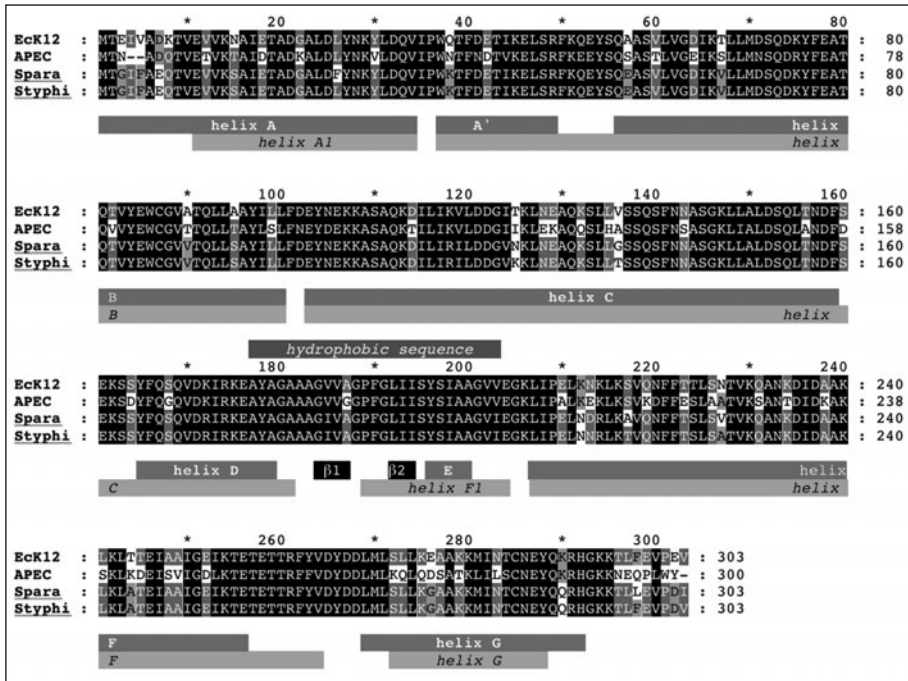


Figure 2. Alignments of HlyE sequences. Sequences from *E. coli* K12 (EcK12), avian *E. coli* (APEC), *Salmonella* Paratyphi (Spara) and *Salmonella* Typhi (Styphi) are shown. Conserved residues are shown in white letters on a black background, residues identical in only three or two sequences as black letters on grey and light grey backgrounds respectively and others as black letters on white background. Red bars below the sequences indicate the positions of alpha helices A to G and black bars show the positions of strands  $\beta 1$  and  $\beta 2$  in the soluble form. Cyan bars show the positions of the helices in the pore form. The hydrophobic putative transmembrane sequence is indicated by the labelled green bar above the sequences. A color version of this image is available at [www.landesbioscience.com/curie](http://www.landesbioscience.com/curie)

redox state of the protein (dithiol, in the cytoplasm and outer membrane vesicles; or disulphide, in the periplasm) affects the oligomeric state of HlyE,<sup>23,25</sup> but more recently both reduced and oxidized HlyE have been shown to be active.<sup>26</sup> At the other end of the rod there is a subdomain (the head domain) that consists of a short two-stranded hydrophobic antiparallel  $\beta$ -sheet flanked by two short helices, known as the  $\beta$ -tongue<sup>9</sup> (Fig. 1). These  $\beta$  strands form part of the 20-residue hydrophobic sequence (Fig. 2) that had previously been predicted to be a transmembrane helix in HlyE.<sup>24</sup> Site-directed mutagenesis has shown that the hydrophobic nature of the  $\beta$ -tongue has to be maintained to allow HlyE to bind to and lyse target cells.<sup>9,23</sup> Host cells are disrupted by the formation of pores in target membranes.<sup>9</sup>

### Oligomerization in Solution

In the crystal, *E. coli* HlyE molecules form dimers that conceal the hydrophobic  $\beta$ -tongue against a second hydrophobic patch lower down the molecule, which may indicate a possible means of maintaining solubility of the toxin in aqueous media.<sup>9</sup> Although initial gel filtration experiments suggested that HlyE is a monomer in solution,<sup>9</sup> more recent investigations have suggested that dimerization—and indeed further oligomerization—occurs in aqueous solution,<sup>23</sup> but that higher order oligomers formed this way are inactive.

### ***Electron Microscopy of HlyE Pores***

The first electron micrographs of the toxin<sup>9</sup> (Fig. 3) revealed that HlyE oligomerizes in the presence of lipid to form circular pores in which the toxin molecules appear to be arranged with their long axes perpendicular to the membrane surrounding a central channel approximately 50 Å in maximum internal diameter. The pore was estimated to contain eight or more HlyE subunits, with a total molecular mass of 250-300 kDa. These initial electron micrographs of the pores were consistent with simple pore models assembled from multiple copies of the soluble HlyE structure, suggesting that HlyE might not undergo large conformational changes during pore formation.<sup>9</sup> However, two recent electron microscopic three-dimensional reconstructions of HlyE pores have revealed that the pores are significantly longer (ca. 140 Å compared with 100 Å) than the water-soluble form of the protein, indicating that conformational changes must take place in order to form a functional pore.<sup>26,27</sup> Although both reconstructions were generated from very similar objects, the interpretation of the data has led to the conclusion that the HlyE pore was octameric in one case<sup>27</sup> and 13-meric in the other.<sup>26</sup> The reason for the discrepancy is unclear.

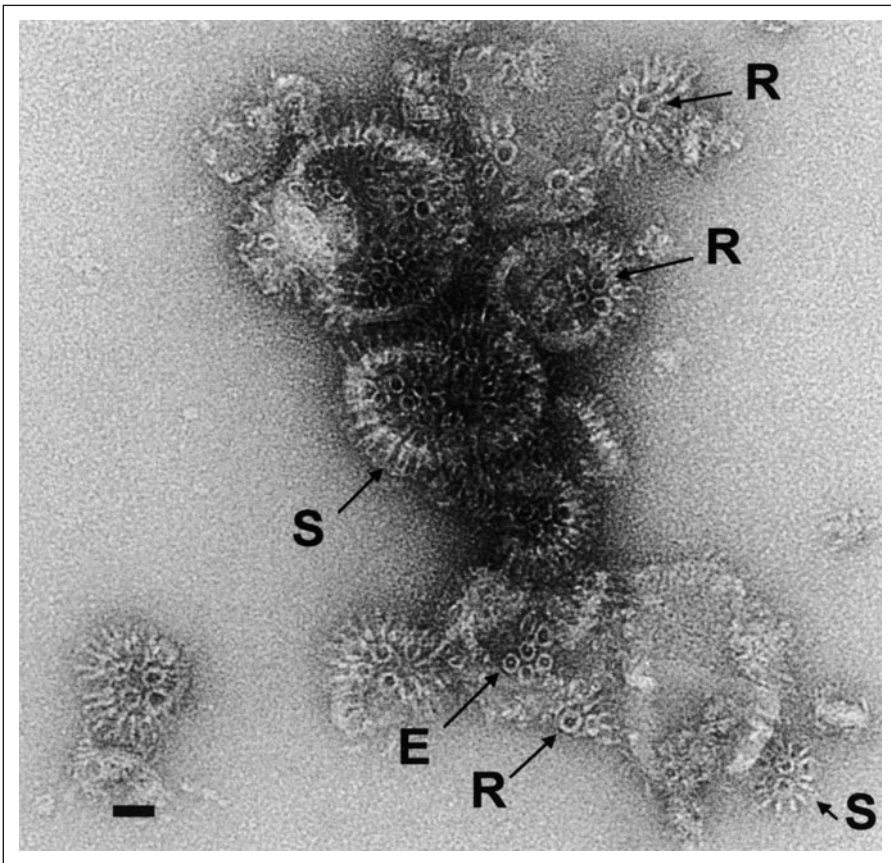


Figure 3. Electron Micrograph of HlyE in lipid vesicles. The micrograph shows negatively stained vesicles containing HlyE with the more heavily stained regions appearing darker. Stain-filled rings (R) are apparent in views parallel to the membrane normal. Some complexes show a central stain-excluding density (E). Side views of the protein complexes are visible at the folded edges of the vesicles as protruding spikes (S). Scale bar (lower left) represents 200 Å. Reproduced from Wallace AJ et al. *Cell* 2000; 100:265-276;<sup>9</sup> with permission from Elsevier.

### Models of the Pore Structure

Both Hunt et al<sup>28</sup> and Eifler et al<sup>26</sup> proposed a model of pore formation in which membrane bound HlyE monomers undergo a rate-limiting conformational change that precedes formation of a functional pore. The latter authors suggested that the  $\beta$ -tongue region of HlyE may form a 26-standed antiparallel  $\beta$  barrel cap structure as part of the process of insertion into the membrane.<sup>26</sup> However it was not suggested that this would comprise the final pore structure and indeed it was unlikely to be so, as there is no  $\beta$  barrel-like peptide sequence at any point in the primary structure of HlyE.<sup>9</sup> Thus, Parker and Feil (2005) have argued that the transmembrane portion of HlyE is almost certainly helical.<sup>29</sup>

A possible model which attempted to reconcile the probable  $\alpha$  helical structure of the transmembrane sequence with the electron microscopic evidence for an elongated pore was proposed by Hunt et al<sup>28</sup> (Fig. 4A). Partial proteolysis of the water-soluble and oligomeric forms of HlyE was employed to identify the inner and outer surfaces of the HlyE pore and the results from this were combined with the structural features from the three-dimensional reconstructions.<sup>26,27</sup> The orientations of the monomers suggested by the pattern of proteolysis implied that the hydrophobic  $\beta$ -tongue is outward facing and thus has the potential to interact with the lipid tails of a target membrane bilayer. However, both electron microscopy studies indicated a substantially longer pore (~140 Å) than that of the model shown in Figure 4 (~100 Å).

Some of the discrepancy in pore length was accounted for in a more sophisticated model (Fig. 4D) that incorporates a rearrangement in the HlyE head domain.<sup>28</sup> In the crystal structure of the soluble form of the toxin, the head domain commences with the amphipathic helix  $\alpha$ D, continues

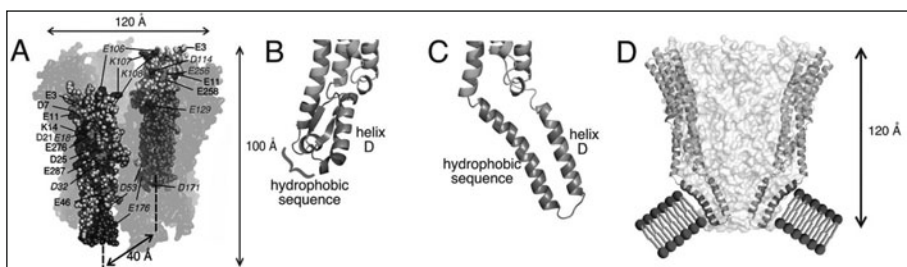


Figure 4. Proposed preliminary models of an octameric HlyE pore. A) A view is shown of a simple space-filling model of an octameric pore assembly illustrating the relative orientations of the HlyE protomers. Six of the protomers are made semi-transparent to give a clear view of the remaining two, chosen to show the positions of the proteolytic cleavage points on the outside (left protomer) and inside (right protomer) of the assembly. The 24-residue hydrophobic sequence that includes the  $\beta$ -tongue, which is required for membrane binding, is coloured dark grey. The C-terminal G helix is coloured light blue. Proteolytic cleavage sites observed in both the water-soluble and oligomeric forms of HlyE are coloured green and labelled in black, cleavage sites protected in the oligomer are coloured and labelled in purple italics and the residue (Asp21) that is sensitive in the oligomer, but not in the water-soluble form of HlyE, is coloured and labelled in dark blue. Approximate dimensions of the proposed assembly are indicated. B) Structure of the head domain of HlyE with the hydrophobic residues in grey and the hydrophilic ones in orange; the hydrophobic putative transmembrane sequence including the  $\beta$ -tongue is on the left, the amphipathic (orange and grey) helix D is on the right; part of the main body of the protomer is in cyan. C) Model in which the hydrophobic sequence becomes a single transmembrane helix (grey, left) which is connected at its N-terminal end to the main body of the protomer via a realigned amphipathic helix D (orange and grey, right). D) The hydrophilic face of helix D (shown entirely in orange for clarity) can then form the inner lining of a pore, while its hydrophobic face packs against the new transmembrane helix (grey) which interacts with lipid (shown schematically). Diagram was produced using PyMOL.<sup>48</sup> Adapted from Hunt S et al. *Microbiology* 2008; 154:633-642;<sup>28</sup> with permission from the Society for General Microbiology. A color version of this image is available at [www.landesbioscience.com/curie](http://www.landesbioscience.com/curie).

through the long hydrophobic sequence which comprises the C-terminal end of  $\alpha$ D, the  $\beta$ -tongue and the short helix  $\alpha$ E and ends just before the commencement of helix  $\alpha$ F which is part of the main body of the molecule (Figs. 1, 2 and 4B).<sup>9</sup> It was proposed that by rearrangement of this region of HlyE the amphipathic helix  $\alpha$ D could form an octameric  $\alpha$ -helical barrel pore,<sup>28</sup> similar to that observed in the C-terminus of *E. coli* Wza,<sup>30</sup> with the hydrophobic residues facing outwards towards the membrane lipids (Fig. 4C,D). It was argued that the proposed rearrangement would be facilitated if the long hydrophobic sequence (previously predicted to be a transmembrane  $\alpha$  helix<sup>24</sup>) were to undergo a conformational change into an  $\alpha$  helix which then returns to the original side of the membrane (Fig. 4C,D). It was suggested that the resulting hydrophobic helix would make favourable interactions with the outward facing side chains of the  $\alpha$  helical barrel and with the lipid bilayer (Fig. 4D).<sup>28</sup>

### Crystal Structure of the Pore Form

The speculation regarding the organization of the HlyE pore was resolved very recently when Ban and coworkers<sup>31</sup> published the 3.3 Å resolution crystal structure of a detergent-stabilised soluble pore-form of HlyE. This revealed that the assembly is a dodecameric pore with a height of 130 Å and a maximum outer diameter of 105 Å (Fig. 5A,B), although given the variability in pore sizes as observed by EM,<sup>26,27</sup> other oligomeric states and conformations may also be possible.

The pore structure shows that major conformational changes take place between the soluble and pore forms of the HlyE protomers<sup>31</sup> (Figs. 2 and 5C,D). Although part of the hydrophobic region around the  $\beta$ -tongue and helix E does indeed refold to become a transmembrane  $\alpha$ -helix as previously proposed,<sup>28</sup> this is accompanied by far more radical changes in the structure of the protomer than had been previously envisaged (Fig. 5C,D), but nevertheless foreshadowed by fluorescence energy transfer, intrinsic fluorescence and site-directed mutagenesis experiments implicating rearrangements of the tail domain during pore formation.<sup>23,24,26,28</sup> C-terminal to the hydrophobic region the changes are relatively modest: the new helix formed from  $\beta$ 2 and  $\alpha$ E (" $\alpha$ F1") forms an N-terminal extension to  $\alpha$ F and in addition there is a change in the location of the turn between the two last helices resulting in a 5-residue lengthening of  $\alpha$ F at its C-terminal end and a concomitant shortening of  $\alpha$ G. N-terminal to the hydrophobic region, however, there are more profound changes: helices  $\alpha$ C and  $\alpha$ D and strand  $\beta$ 1 become one continuous helix, as do

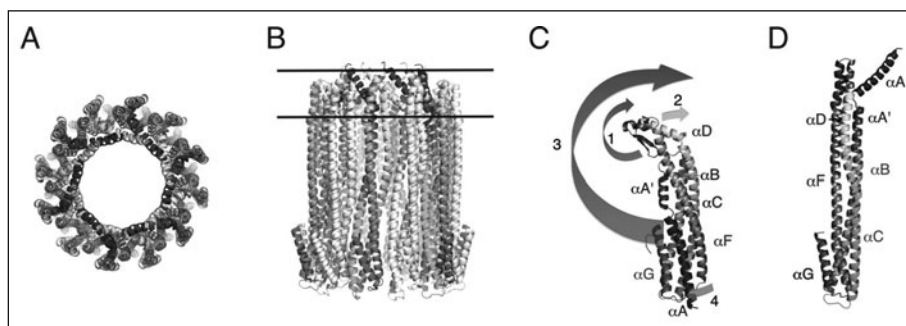


Figure 5. The structure of the pore form of HlyE.<sup>31</sup> Views of the dodecameric pore complex from (A) above and (B) from the side, with alternate protomers white and coloured; horizontal lines represent the proposed position of a target membrane. C) View of the HlyE protomer in the soluble form<sup>9</sup> and (D) in the pore. In (C) numbered arrows schematically summarize the proposed sequence of changes: (1) movement of the  $\beta$ -tongue to become a hydrophobic extension of helix  $\alpha$ D; (2)  $\alpha$ D to  $\beta$ 1 becomes a helical extension to  $\alpha$ C and  $\beta$ 2 to  $\alpha$ E becomes a helical extension to  $\alpha$ F; (3) movement of  $\alpha$ A and  $\alpha$ A' to the other end of the protomer and (4) movement of  $\alpha$ F into the space left by  $\alpha$ A. Diagrams are coloured and labelled as Figure 1 and produced using PyMOL.<sup>48</sup> A color version of this image is available at [www.landesbioscience.com/curie](http://www.landesbioscience.com/curie).

helices  $\alpha$ B and  $\alpha$ A' (the final section of  $\alpha$ A). As a result of this,  $\alpha$ A is rotated by approximately  $180^\circ$  (and the N-terminus moves 140 Å) relative to its position in the soluble form and thus becomes situated at the opposite end of the protomer (Fig. 5C,D). The consequence of all these changes is that the main body of the protomer becomes an elongated three-helix bundle<sup>31</sup> in contrast to the four-helix bundle observed in the soluble form of the toxin.<sup>9</sup> New molecular surfaces are formed by these rearrangements and allow the formation of a network of 25 hydrogen bonds and 13 salt bridges between each pair of protomers in the pore.<sup>31</sup>

The dramatically relocated  $\alpha$ A helices from the 12 protomers form a cone-shaped  $\alpha$ -helical barrel inside the pore and it is this that defines the  $\sim 30$  Å limiting diameter of the pore (Fig. 5A,B).<sup>31</sup> The outer part of this  $\alpha$ -helical barrel is hydrophobic and it is proposed that this together with the hydrophobic sequence around  $\alpha$ F1 insert into and form the interface with the membrane (Fig. 5).

This remarkable new structure of an HlyE pore resolves many of the issues around the mechanism of pore formation by this toxin and allows proposal of a detailed possible mechanism for membrane insertion,<sup>31</sup> which is discussed further below.

## Process of Membrane Insertion

HlyE-mediated cell lysis is the product of a complex series of steps in which HlyE must recognize and bind to the target cell and then assemble to form a functional pore. The data presented by Hunt et al (2008)<sup>28</sup> suggest that conversion of HlyE from a water-soluble dimer,<sup>9,32</sup> in which the hydrophobic surfaces in the head ( $\beta$ -tongue) and tail (residues of helices B, C and G) are shielded from the solvent, to a monomer that can bind to a target membrane is fast. The fluorescence energy transfer experiments suggest that after interaction with a membrane HlyE protomers rapidly begin to oligomerize.<sup>28</sup> Thus, it is suggested that neither membrane binding, nor initial interactions between membrane bound HlyE monomers are rate-limiting steps in creating a functional pore. Nevertheless, during these rapid phases HlyE undergoes conformational changes in regions including those (for example the tail region) that are remote from the  $\beta$ -tongue, which is essential for interaction with a membrane.<sup>9,24</sup> The changes in HlyE conformation were suggested to be required for binding the membrane and facilitating subsequent initial interactions between HlyE protomers to form parallel membrane bound HlyE molecules in a prepore structure. This rapid phase is then followed by a slow component, most apparent as a temperature-dependent lag phase, with relatively high activation energy, before hemolysis occurs. Taken together these observations indicate that whereas HlyE binding to a target and initial oligomerization are rapid, functional pore-formation is a much slower process. Such a mechanism accounts for the relatively poor hemolysis observed at  $15^\circ\text{C}$  compared to  $37^\circ\text{C}$  and the need for prolonged incubation to observe cell lysis at low HlyE concentrations. Thus, the data presented by Hunt et al<sup>28</sup> broadly support the conclusions of Eiffler et al,<sup>26</sup> who also suggested that there is a rate-limiting conformational transition in membrane bound HlyE that precedes the formation of a functional pore.

The availability of structures of the soluble HlyE monomer<sup>9</sup> and the recent description of an HlyE pore<sup>31</sup> has allowed the proposal of a detailed model for membrane insertion.<sup>31</sup> In this model the trigger for the structural change (Fig. 5C,D) involves Phe 190 at the tip of the  $\beta$ -tongue which, in the soluble form, interacts with four other aromatic residues (Phe 50, Tyr 54, Phe 159 and Tyr 165).<sup>9</sup> It is envisioned that in proximity to the membrane Phe 190 and the  $\beta$ -tongue flip out into the lipid bilayer. The removal of Phe 190 destabilizes the cluster of aromatic residues and precipitates the rearrangements of the protomer associated with the transition to the pore form. In these rearrangements helix  $\alpha$ D and the first half of the hydrophobic sequence including  $\beta$ 1 become an extension of  $\alpha$ C;  $\alpha$ A' becomes an extension of  $\alpha$ B and the amphipathic  $\alpha$ A relocates towards and attaches to the membrane; and finally  $\alpha$ F, extended by  $\beta$ 2 and  $\alpha$ E at one end and part of  $\alpha$ G at the other, takes the place vacated by  $\alpha$ A. This refolded protomer is attached to the membrane and then acts as a nucleation site for the recruitment of more protomers. When a complete prepore is assembled on the membrane it is proposed that the target membrane becomes distorted and insertion of  $\alpha$ A and  $\alpha$ F into the lipid bilayer takes place to form the functional pore.<sup>31</sup>

## HlyE Secretion and Exploitation in Vaccine Development and Tumour Targeting

HlyE is a remarkable protein in that it lacks previously recognized protein export signal sequences yet is translocated from the bacterial cytoplasm without modification to the periplasm, where it accumulates.<sup>3,23,25,33,34</sup> The association between extracellular HlyE and periplasmic proteins has led to speculation that HlyE may be secreted via outer membrane vesicles.<sup>34</sup> This theory is further supported by the observation by the Uhlin group that HlyE protein is exposed on the surface of the *E. coli* cell, as demonstrated by immunofluorescence, electron microscopy (EM) and atomic force microscopy (AFM).<sup>25</sup> The latter studies revealed small outer-membrane vesicles surrounding the bacterial cells containing HlyE-like assemblies, resembling those described by Wallace et al (2000),<sup>9</sup> were observed in vesicles from the HlyE-expressing strains.<sup>25</sup> These were confirmed as HlyE by immunolocalisation using anti-HlyE antibodies in the immunogold labelling method. However, it is evident that there is still much to learn about the mechanism of HlyE export, but this gap in our knowledge has not inhibited attempts to exploit the properties of HlyE in the design of new vaccines and as a potential therapeutic gene.

Delivery of foreign antigens to induce protective immune responses using live attenuated bacteria is an exciting area of vaccine development. Because surface-exposed or secreted antigens are more immunogenic than cytoplasmic antigens, attention has been drawn to HlyE as an export system for displaying foreign antigens in attenuated *S. Typhi* strains. Taking advantage of the ability of HlyE to facilitate the export of proteins fused at its C-terminus, strains of *S. Typhi* engineered to express several antigens (including: protective *Bacillus anthracis* antigens; and the *Plasmodium falciparum* truncated circumsporozoite surface protein) have been reported to have potential as vaccine candidates.<sup>35-38</sup> One of the perceived advantages of these strains is that they do not require additional engineering to incorporate a secretion system, which might have a detrimental effect on the strain, because HlyE is readily exported by *S. Typhi*.

The targeting of HlyE to outer membrane vesicles has been used to localize active proteins, again as HlyE fusions, to outer membrane vesicles with the aim of mapping the progress of HlyE-containing vesicles during infection of host cells and for biotechnology applications such as surface display and delivery of therapeutic proteins.<sup>39</sup> Also, the cytotoxic properties of HlyE overproduced by attenuated *S. Typhimurium* have been exploited in combination with an engineered hypoxia-regulated promoter to increase necrosis and inhibit growth of tumours in mice.<sup>40</sup>

## HlyE-Like Toxins from *Bacillus cereus*

Sequence comparisons suggest that HlyE toxins form a small isolated family of virulence factors restricted to the closely related organisms *E. coli*, *S. flexneri* and *S. Typhi* and *S. Paratyphi*. Moreover, until very recently, the X-ray crystal structure of HlyE appeared to exhibit a unique overall three-dimensional fold, based on searches of the structural databases.<sup>9</sup> However, even though there is little sequence homology, very recent structural work has revealed a striking three-dimensional fold resemblance between HlyE and a family of pore-forming toxins from the Gram-positive bacterium *B. cereus*.<sup>41,42</sup>

The Gram-positive bacterium *Bacillus cereus* possesses three putative enterotoxins: hemolysin BL (Hbl), nonhaemolytic enterotoxin (Nhe) and cytotoxin K (CytK). Hbl and Nhe are tripartite toxins and are encoded by three genes cotranscribed as operons in which *hblCDA* encodes Hbl components L<sub>2</sub>, L<sub>1</sub> and B and *nheABC* encodes NheA, NheB and NheC (reviewed in Arnesen et al (2008).)<sup>43</sup> There is sequence homology between the three components in each complex and between the proteins of Nhe and Hbl.<sup>42</sup> Recently, the X-ray crystal structure of the B component of hemolysin BL from *B. cereus* was published;<sup>41</sup> despite low sequence homology, it was discovered that *B. cereus* Hbl-B shared significant structural similarities with *E. coli* HlyE<sup>41,42</sup> (Fig. 6). Both the HlyE and the hemolysin BL structures are based on elongated four-helix bundles with a simple square, left-handed, up-down-up-down arrangement of helices.<sup>44</sup> This is a fairly commonly encountered folding topology<sup>45</sup> and so this similarity is not sufficient to allow the inference of an evolutionary



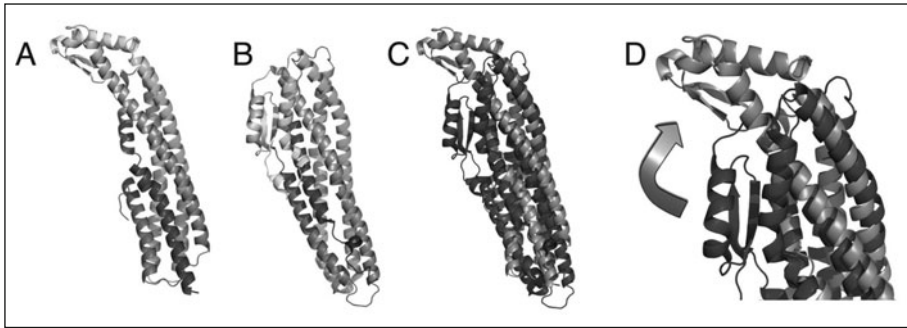


Figure 6. Comparison of *E. coli* HlyE and *B. cereus* Hbl-B structures. A) and B) are cartoons of HlyE and Hbl-B respectively (both rainbow coloured as Fig. 1). C) shows a superposition of HlyE (orange) and Hbl-B (dark blue).<sup>41,42</sup> D) is a detail of (C) showing the different positions occupied by the head domains in the two protein structures, the arrow indicating the relative displacement between Hbl-B and HlyE. Diagram was produced using PyMOL.<sup>48</sup> A color version of this image is available at [www.landesbioscience.com/curie](http://www.landesbioscience.com/curie).

relationship. What is far more significant, however, is that the folds of the tail domains and of the head domains of both proteins are also very similar,<sup>41,42</sup> even though the folding topologies of the two domains had previously been thought to be unique to HlyE.<sup>9</sup> Moreover, as with HlyE, the single long hydrophobic sequence in Hbl-B is located in the region of the  $\beta$  hairpin in the head domain. One difference is that the orientation of the head domain with respect to the tail domain differs appreciably between the two proteins (Fig. 6).<sup>41,42</sup> In the crystal structure of Hbl-B, the head domain is oriented so that it interacts with the main four helix bundle and with the tail domain ( $\sim 30^\circ$  interdomain angle), which itself has a longer C-terminal helix.<sup>41</sup> In contrast, in HlyE<sup>9</sup> the head domain makes relatively few interactions with the rest of the molecule ( $\sim 120^\circ$  interdomain angle). Interestingly, the alternate orientations of the head domains in the crystal structures of HlyE and HBL-B (Fig. 6) suggests a degree of flexibility in this region that is consistent with the proposed rearrangements of the head domain and  $\beta$ -tongue in the first steps of model of the HlyE pore formation proposed by Mueller et al.<sup>31</sup>

Hardy, Granum and coworkers have shown Nhe to be cytotoxic to Caco-2 and Vero cells, to form pores in planar lipid bilayers and to be haemolytic against erythrocytes.<sup>42</sup> Based on the significant sequence similarities to Hbl-B, it was also possible to generate three-dimensional homology models for NheB and NheC:<sup>42</sup> both contain a predicted hydrophobic segment that correlates with the  $\beta$ -hairpin seen in HlyE and Hbl-B. The structural and functional similarities among Nhe, Hbl and HlyE may indicate that they belong to a superfamily of pore-forming toxins.<sup>42</sup> As more X-ray crystal structures are determined, it is possible that the number of HlyE homologues identified will increase and so it will become apparent if HlyE, Hbl and Nhe are truly members of a larger superfamily of pore-forming toxins.

## Conclusion

Although discovered relatively recently, the importance of HlyE is becoming apparent. The confirmation of involvement in *Salmonella* virulence<sup>15,46,47</sup> and the presence of homologues in many *E. coli* strains including avian pathogenic *E. coli* (APEC),<sup>10,11</sup> suggests that HlyE is a versatile virulence factor that contributes to the establishment of a range of infections. Moreover the clear structural resemblances between HlyE and the Hbl and Nhe toxins of *Bacillus cereus* indicate that these proteins are members of a broader superfamily of pore-forming toxins. Furthermore, the availability of structures for both soluble and pore forms of HlyE represents a major step forward in the understanding of  $\alpha$ -helical pore forming toxins in general.

## References

1. del Castillo FJ, Leal SC, Moreno F et al. The *Escherichia coli* K-12 sheA gene encodes a 34-kDa secreted haemolysin. *Mol Microbiol* 1997; 25:107-115.
2. Green J, Baldwin ML. The molecular basis for the differential regulation of the hlyE-encoded haemolysin of *Escherichia coli* by FNR and HlyX lies in the improved Activating Region 1 contact of HlyX. *Microbiology* 1997; 143:3785-3793.
3. Ludwig A, Bauer S, Benz R et al. Analysis of the SlyA-controlled expression, subcellular localization and pore-forming activity of a 34 kDa haemolysin (ClyA) from *Escherichia coli* K-12. *Mol Microbiol* 1999; 31:557-567.
4. Ludwig A, von Rhein C, Bauer S et al. Molecular analysis of cytolysin a (ClyA) in pathogenic *Escherichia coli* strains. *J Bacteriol* 2004; 186:5311-5320.
5. Oscarsson J, Mizunoe Y, Uhlin BE et al. Induction of haemolytic activity in *Escherichia coli* by the slyA gene product. *Mol Microbiol* 1996; 20:191-199.
6. Oscarsson J, Westermark M, Lofdahl S et al. Characterization of a pore-forming cytotoxin expressed by *Salmonella enterica* serovars Typhi and Paratyphi A. *Infect Immun* 2002; 70:5759-5769.
7. Lai XH, Arencibia I, Johansson A et al. Cytocidal and apoptotic effects of the ClyA protein from *Escherichia coli* on primary and cultured monocytes and macrophages. *Infect Immun* 2000; 68:4363-4367.
8. Soderblom T, Oxhamre C, Wai SN et al. Effects of the *Escherichia coli* toxin cytolysin A on mucosal immunostimulation via epithelial Ca<sup>2+</sup> signalling and Toll-like receptor 4. *Cell Microbiol* 2005; 7:779-788.
9. Wallace AJ, Stillman TJ, Atkins A et al. *E. coli* hemolysin E (HlyE, ClyA, SheA): X-ray crystal structure of the toxin and observation of membrane pores by electron microscopy. *Cell* 2000; 100:265-276.
10. Reingold J, Starr N, Maurer J et al. Identification of a new *Escherichia coli* She haemolysin homolog in avian *E. coli*. *Vet Microbiol* 1999; 66:125-134.
11. Nagai S, Yagihashi T, Ishihama A. An avian pathogenic *Escherichia coli* strain produces a hemolysin, the expression of which is dependent on cyclic AMP receptor protein gene function. *Vet Microbiol* 1998; 60:227-238.
12. Coote JG. Structural and functional relationships among the RTX toxin determinants of Gram negative bacteria. *FEMS Microbiol Rev* 1992; 88:137-162.
13. Kerenyi M, Allison HE, Batai I et al. Occurrence of hlyA and sheA genes in extraintestinal *Escherichia coli* strains. *J Clin Microbiol* 2005; 43(6):2965-2968.
14. Faucher SP, Forest C, Beland M et al. A novel PhoP-regulated locus encoding the cytolysin ClyA and the secreted invasin TaiA of *Salmonella enterica* serovar Typhi is involved in virulence. *Microbiology* 2009; 155:477-488.
15. von Rhein C, Hunfeld KP, Ludwig A. Serologic evidence for effective production of cytolysin A in *Salmonella enterica* serovars Typhi and Paratyphi A during human infection. *Infect Immun* 2006; 74:6505-6508.
16. von Rhein C, Bauer S, Sanjurjo EJM et al. ClyA cytolysin from *Salmonella*: Distribution within the genus, regulation of expression by SlyA and pore-forming characteristics. *Int J Med Microbiol* 2009; 299:21-35.
17. Hight AR, Berry AM, Bettelheim KA et al. The frequency of molecular detection of virulence genes encoding cytolysin A, high-pathogenicity island and cytolethal distending toxin of *Escherichia coli* in cases of sudden infant death syndrome does not differ from that in other infant deaths and healthy infants. *J Med Microbiol* 2009; 58:285-289.
18. von Rhein C, Bauer S, Simon V et al. Occurrence and characteristics of the cytolysin A gene in *Shigella* strains and other members of the family Enterobacteriaceae. *FEMS Microbiol Lett* 2008; 287:143-148.
19. Wyborn NR, Stapleton MR, Norte VA et al. Regulation of *Escherichia coli* hemolysin E expression by H-NS and *Salmonella* SlyA. *J Bacteriol* 2004; 186:1620-1628.
20. Westermark M, Oscarsson J, Mizunoe Y et al. Silencing and activation of ClyA cytotoxin expression in *Escherichia coli*. *J Bacteriol* 2000; 182:6347-6357.
21. Lithgow JK, Haider F, Roberts IS et al. Alternate SlyA and H-NS nucleoprotein complexes control hlyE expression in *Escherichia coli* K-12. *Mol Microbiol* 2007; 66:685-698.
22. Zhao G, Weatherspoon N, Kong W et al. A dual-signal regulatory circuit activates transcription of a set of divergent operons in *Salmonella typhimurium*. *Proc Natl Acad Sci USA* 2008; 105:20924-20929.
23. Atkins A, Wyborn NR, Wallace AJ et al. Structure-function relationships of a novel bacterial toxin, hemolysin E—The role of alpha(G). *J Biol Chem* 2000; 275:41150-41155.
24. Oscarsson J, Mizunoe Y, Li L et al. Molecular analysis of the cytolytic protein ClyA (SheA) from *Escherichia coli*. *Mol Microbiol* 1999; 32:1226-1238.
25. Wai SN, Lindmark B, Soederblom T et al. Vesicle-mediated export and assembly of pore-forming oligomers of the enterobacterial ClyA cytotoxin. *Cell* 2003; 115:25-35.

26. Eifler N, Vetsch M, Gregorini M et al. Cytotoxin ClyA from *Escherichia coli* assembles to a 13-meric pore independent of its redox-state. *EMBO J* 2006; 25:2652-2661.
27. Tzokov SB, Wyborn NR, Stillman TJ et al. Structure of the hemolysin E (HlyE, ClyA and SheA) channel in its membrane-bound form. *J Biol Chem* 2006; 281:23042-23049.
28. Hunt S, Moir AJG, Tzokov S et al. The formation and structure of *Escherichia coli* K-12 haemolysin E pores. *Microbiology* 2008; 154:633-642.
29. Parker MW, Feil SC. Pore-forming protein toxins: from structure to function. *Prog Biophys Mol Biol* 2005; 88:91-142.
30. Dong CJ, Beis K, Nesper J et al. Wza the translocon for *E. coli* capsular polysaccharides defines a new class of membrane protein. *Nature* 2006; 444:226-229.
31. Mueller M, Grauschkopf U, Maier T et al. The structure of a cytolytic alpha-helical toxin pore reveals its assembly mechanism. *Nature* 2009; 459:726-730.
32. Wyborn NR, Clark A, Roberts RE et al. Properties of haemolysin E (HlyE) from a pathogenic *Escherichia coli* avian isolate and studies of HlyE export. *Microbiology* 2004; 150:1495-1505.
33. Ludwig A, Tengeli C, Bauer S et al. SlyA, a regulatory protein from *Salmonella typhimurium*, induces a haemolytic and pore-forming protein in *Escherichia coli*. *Mol Gen Genet* 1995; 249:474-486.
34. del Castillo FJ, Moreno F, del Castillo I. Secretion of the *Escherichia coli* K-12 sheA hemolysin is independent of its cytolytic activity. *FEMS Microbiol Lett* 2001; 204:281-285.
35. Galen JE, Zhao LC, Chinchilla M et al. Adaptation of the endogenous *Salmonella enterica* serovar typhi clyA-encoded hemolysin for antigen export enhances the immunogenicity of anthrax protective antigen domain 4 expressed by the attenuated live-vector vaccine strain CVD 908-htrA. *Infect Immun* 2004; 72:7096-7106.
36. Stokes MGM, Titball RW, Neeson BN et al. Oral administration of a *Salmonella enterica*-based vaccine expressing *Bacillus anthracis* protective antigen confers protection against aerosolized B-anthraxis. *Infect Immun* 2007; 75:1827-1834.
37. Baillie LWJ, Rodriguez AL, Moore S et al. Towards a human oral vaccine for anthrax: The utility of a *Salmonella Typhi* Ty21a-based prime-boost immunization strategy. *Vaccine* 2008; 26:6083-6091.
38. Chinchilla M, Pasetti MF, Medina-Moreno S et al. Enhanced immunity to *Plasmodium falciparum* circumsporozoite protein (PfCSP) by using *Salmonella enterica* serovar Typhi expressing PfCSP and a PfCSP-encoding DNA vaccine in a heterologous prime-boost strategy. *Infect Immun* 2007; 75:3769-3779.
39. Kim JY, Doody AM, Chen DJ et al. Engineered bacterial outer membrane vesicles with enhanced functionality. *J Mol Biol* 2008; 380:51-66.
40. Ryan RM, Green J, Hunt S et al. Bacterial delivery of a novel cytolysin to hypoxic areas of solid tumors. *Gene Ther* 2009; 16:329-339.
41. Madegowda M, Eswaramoorthy S, Burley SK et al. X-ray crystal structure of the B component of Hemolysin BL from *Bacillus cereus*. *Proteins Struct Funct Bioinform* 2008; 71:534-540.
42. Fagerlund A, Lindback T, Storset AK et al. *Bacillus cereus* Nhe is a pore-forming toxin with structural and functional properties similar to the ClyA (HlyE, SheA) family of haemolysins, able to induce osmotic lysis in epithelia. *Microbiology* 2008; 154:693-704.
43. Arnesen LPS, Fagerlund A, Granum PE. From soil to gut: *Bacillus cereus* and its food poisoning toxins. *FEMS Microbiology Reviews* 2008; 32:579-606.
44. Presnell SR, Cohen FE. Topological distribution of 4 alpha helix bundles. *Proc Natl Acad Sci USA* 1989; 86:6592-6596.
45. Harris NL, Presnell SR, Cohen FE. 4 helix bundle diversity in globular proteins. *J Mol Biol* 1994; 236:1356-1368.
46. Ansong C, Yoon H, Norbeck AD et al. Proteomics analysis of the causative agent of typhoid fever. *J Proteome Res* 2008; 7:546-557.
47. Fuentes JA, Villagra N, Castillo-Ruiz M et al. The *Salmonella typhi* hlyE gene plays a role in invasion of cultured epithelial cells and its functional transfer to *S. typhimurium* promotes deep organ infection in mice. *Res Microbiol* 2008; 159:279-287.
48. DeLano WL, Lam JW. PyMOL: A communications tool for computational models. *Abstracts of Papers of the American Chemical Society* 2005; 230:254-COMP.